PHYSICAL REVIEW B **74**, 224435 (2006)

Comparison between disordered quantum spin-$\frac{1}{2}$ chains

C. A. Lamas,[1] D. C. Cabra,[1,2,3] M. D. Grynberg,[1] and G. L. Rossini[1]
[1]*Departamento de Física, Universidad Nacional de La Plata, C.C. 67, 1900 La Plata, Argentina*
[2]*Laboratoire de Physique Théorique, Université Louis Pasteur, 3 Rue de l'Université, 67084 Strasbourg, Cédex, France*
[3]*Facultad de Ingeniería, Universidad Nacional de Lomas de Zamora, Cno. de Cintura y Juan XXIII, (1832) Lomas de Zamora, Argentina*

(Received 20 July 2006; revised manuscript received 6 October 2006; published 27 December 2006)

We study the magnetic properties of two types of one-dimensional *XX* spin-$\frac{1}{2}$ chains. The first type has only nearest-neighbor interactions which can be either antiferromagnetic or ferromagnetic, and the second type has both nearest-neighbor and next-nearest-neighbor interactions, but only antiferromagnetic in character. We study these systems in the presence of low magnetic fields both analytically and numerically. Comparison of results shows a close relation between the two systems, which is in agreement with results previously found in Heisenberg chains by means of a numerical real-space renormalization-group procedure.

DOI: 10.1103/PhysRevB.74.224435 PACS number(s): 75.10.Jm, 75.10.Nr, 75.40.Mg

I. INTRODUCTION

One-dimensional quantum spin systems have been extensively studied over the last years.[1] In particular, randomness has a profound effect on their physical properties and is always present in real systems through impurities or structural disorder. It can even produce singular behaviors in the magnetic properties, not observed in pure systems. The study of disordered systems has thus attracted a lot of attention from both experimental and theoretical sides. In particular, when quenched disorder dominates the large-scale physics, two kinds of situations arise: the system scales either to an infinite disorder fixed point, such as in the case of the random antiferromagnetic $S=1/2$ Heisenberg chain, or to a strong disorder fixed point, such as Griffiths phases in quantum models (see Ref. 2 for a complete description and references therein). Consequently, one of the main motivations to study disordered quantum spin chains is the possibility of classifying their behavior in universality classes associated with different regions in their phase diagrams.[3,4]

In the last few years, numerical works[3–5] have shown that the thermodynamic properties of disordered Heisenberg chains with nearest-neighbor (NN) and next-nearest-neighbor (NNN) couplings, *both antiferromagnetic*, are very similar to those found in disordered chains with *only* NN couplings which can be *either antiferromagnetic or ferromagnetic*. In fact, it was shown that under the real-space renormalization-group (RSRG) approach introduced in Ref. 6 the former systems flow to a fixed point characterized as a chain with only NN couplings in a given distribution, taking both antiferromagnetic and ferromagnetic values.

More specifically, let us consider a Heisenberg chain with Hamiltonian

$$H=\sum_i (J_i\vec{S}_i\cdot\vec{S}_{i+1}+J_i'\vec{S}_i\cdot\vec{S}_{i+2}), \tag{1}$$

where $\vec{S}_i$ are spin-$\frac{1}{2}$ operators and the couplings $J_i>0$ and $J_i'>0$, both antiferromagnetic, follow the probability distributions $P(J_i)$ and $P(J_i')$. Let us review the arguments of Refs. 3 and 4. If we consider the adjacent spins that are coupled by the strongest bond (say, the spins 3 and 4 in Fig. 1) and its neighbors, we are left with a problem whose Hamiltonian can be written as

$$H=H_0+H_I+H_{rest}, \tag{2}$$

where

$$H_0=J_{34}\vec{S}_3\cdot\vec{S}_4, \tag{3}$$

$$H_I=J_{23}\vec{S}_2\cdot\vec{S}_3+J_{45}\vec{S}_4\cdot\vec{S}_5+J_{35}'\vec{S}_3\cdot\vec{S}_5+J_{24}'\vec{S}_2\cdot\vec{S}_4, \tag{4}$$

and H_{rest} corresponds to all other spins that are not coupled to spins 3 and 4.

The sole consideration of H_0+H_I is enough to determine the effective interaction between the spins 2 and 5, as follows.[4,6,7] The ground state for the Hamiltonian H_0 is a singlet with energy $E_0=-\frac{3}{4}J_{34}$ while excited triplet states have energy $E_1=\frac{1}{4}J_{34}$. Since J_{34} is the largest bond, one can take H_I as a perturbation. Regarding $\vec{S}_2$ and $\vec{S}_5$ as external operators, a second-order perturbation calculation gives an effective Hamiltonian describing the low-energy sector (we consider only the coupling generated between 2 and 5)

$$E=-\frac{3}{4}J_{34}-\frac{3}{16J_{34}}[(J_{23}-J_{24}')^2+(J_{35}'-J_{45})^2]+\frac{(J_{23}-J_{24}')(J_{45}-J_{35}')}{2J_{34}}\vec{S}_2\cdot\vec{S}_5. \tag{5}$$

From this result one can remove the spins $\vec{S}_3$ and $\vec{S}_4$ from the original Hamiltonian, replacing them by an effective NN coupling $\tilde{J}_{25}$,

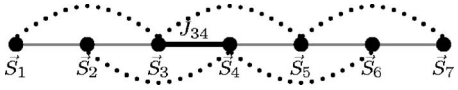

FIG. 1. Schematic picture of a disordered-antiferromagnetic NN-NNN chain.

$$\tilde{J}_{25} = \frac{(J_{23} - J'_{24})(J_{45} - J'_{35})}{2J_{34}}, \tag{6}$$

between $\vec{S}_2$ and $\vec{S}_5$.

Following this RSRG decimation procedure one ends up with a NN spin-$\frac{1}{2}$ chain in which effective interactions like $\tilde{J}_{25}$ can be ferromagnetic. Notice that when the NNN couplings are very weak compared to the NN couplings the ferromagnetic effective interaction is unlikely to appear. On the contrary, for strong NNN couplings, the RSRG method does generate effective ferromagnetic couplings and the system flows to a phase controlled by large effective spins at low energies.[4]

It is the aim of the present paper to further understand the connection between these and related systems in more general situations. In particular we are interested in comparing the magnetic properties of easy-plane *XX* spin-$\frac{1}{2}$ chains in the presence of uniform magnetic fields. Notice, however, that in the Heisenberg model the properties can be often different.[8–10] Even in the pure case, the Heisenberg model exhibits a plateau at $M=1/3$ that is not present in the *XX* model.[11] Related results, like a study of the correlation functions in the random spin-$\frac{1}{2}$ *XX* chain can be found in Ref. 12, whereas a detailed analysis of the Griffiths phase and a phenomenological scaling theory can be found in Ref. 13.

We first study analytically the magnetic properties of quantum *XX* spin-$\frac{1}{2}$ chains with antiferromagnetic and ferromagnetic NN interactions, using an elegant argument relating magnetization with random walk problems[14] (see details in the Appendix). In a second step we implement a numerical self-consistent method based on a mean-field approximation,[15] which allows for analyzing quantum *XX* spin-$\frac{1}{2}$ chains with NN and NNN interactions, to be applied in the antiferromagnetic case. Finally, common features found in these spin systems are discussed.

The structure of the paper is the following. Analytical results derived from the random walk argument are presented in Sec. II for homogeneous and dimerized disorder in antiferromagnetic NN chains, as well as novel results for dimerized distributions of antiferromagnetic and ferromagnetic couplings in NN chains. The self-consistent numerical method is presented in Sec. III, then tested on pure (ordered) NNN antiferromagnetic chains in Sec. IV, and finally applied to the NNN disordered case in Sec. V. Numerical results are compared with exact diagonalization for small chains, up to 24 spins, at each step. The comparison between both types of chains, summary, and conclusions are presented in Sec. VI.

II. ANALYTICAL TREATMENT FOR NN SPIN-$\frac{1}{2}$ CHAINS

In this section we study analytically the magnetization of one-dimensional spin-$\frac{1}{2}$ systems with NN interactions whose Hamiltonian in the *XX* model is

$$H = \sum_i J_i (S_i^x S_{i+1}^x + S_i^y S_{i+1}^y) - h \sum_i S_i^z, \tag{7}$$

where J_i are random nearest-neighbor couplings [either antiferromagnetic (AF) or ferromagnetic (F)] and h is a uniform magnetic field. By means of the Jordan-Wigner transformation[16]

$$S_i^+ \equiv c_i^\dagger e^{i\pi\phi_i},$$

$$S_i^- \equiv e^{-i\pi\phi_i} c_i,$$

$$S_i^z \equiv c_i^\dagger c_i - \frac{1}{2}, \tag{8}$$

where $\phi_i \equiv \Sigma_{l=1}^{i-1} c_l^\dagger c_l$, we can rewrite this Hamiltonian in terms of spinless fermionic operators

$$H = \sum_i t_i (c_i^\dagger c_{i+1} + \text{H.c.}) - h \sum_i c_i^\dagger c_i \tag{9}$$

(in this section we use $t=J/2$). Notice that the magnetic field acts as a chemical potential for the fermions.

We start with the study of the homogeneous disordered case where the couplings follow a homogeneous distribution $[P(t_i)=P(t_j)\,\forall\, i,j]$. Following the argument presented in Ref. 14 one can introduce a random variable v_i which follows a finite-range random-walk evolution between reflecting and absorbing barriers. Details are outlined in the Appendix. The relevant quantity to compute here is the number of one-particle eigenstates, $N(E)$, with energies below E, which for low energies is related to the average number $\bar{n}$ of steps necessary for v_i to complete a diffusion cycle from the reflecting barrier to the absorbing one. The relation between them is[17]

$$N(E) = \frac{1}{2\bar{n}} + \frac{1}{2}. \tag{10}$$

In the present case one gets $\bar{n} \sim (v_{max} - v_{min})^2/\sigma^2$, where σ^2 is the variance of the coupling distribution P and v_{min} and v_{max} are the position of the barriers, rendering

$$N(E) \cong \frac{1}{2}\left(1 + \frac{\sigma^2}{[\ln(\tilde{t}/E)^2]^2}\right), \tag{11}$$

where $\tilde{t}$ is the average of positive AF couplings. This result indeed describes the magnetization of the spin system (7). We write the mean magnetization m in terms of fermionic variables using the Jordan-Wigner transformation

$$m = \left\langle \sum_i S_i^z \right\rangle = \sum_i (\langle c_i^\dagger, c_i \rangle - 1/2), \tag{12}$$

in order to exhibit the relation between magnetization and fermion filling. Recalling that the magnetic field acts as a chemical potential and regulates the fermion filling, for low magnetic field we finally obtain a mean magnetization per site

$$M(h) \sim \frac{1}{2}\left(\frac{\sigma^2}{[\ln(\tilde{t}/h)^2]^2}\right) \tag{13}$$

(here $M=2m/N$, with N the number of spins in the chain, is normalized to 1 at saturation).

Now we turn to the case of dimerized inhomogeneous distributions [$(P_{odd}(t_i)$ for odd sites i different from $P_{even}(t_j)$

for even sites j]. The result above was suitably generalized in Ref. 18 for this case: the random variable u_i undergoes a random walk with diffusion coefficient D and a driving force F given by

$$D = \frac{1}{2}\{\mathrm{var}^2_{odd}[\ln(t_i^2)] + 2\mathrm{var}^2_{even}[\ln(t_j^2)]\}, \tag{14}$$

$$F = \langle \ln(t_i^2)\rangle_{odd} - \langle \ln(t_j^2)\rangle_{even}, \tag{15}$$

where "var" stands for the variance of the corresponding distribution. The average number of steps for a diffusion cycle to be completed behaves now as $\bar{n} \sim e^{\alpha(u_{max}-u_{min})/2}$. Then the magnetization of the system is seen to follow a power law

$$M(h) \sim h^{\alpha}, \tag{16}$$

with $\alpha = \frac{2F}{D}$.

In what follows we generalize this procedure to study the system of interest here—namely, a disordered spin-$\frac{1}{2}$ chain with AF and F NN interactions. Let us consider the following binary coupling distribution:

$$P(t_i) = xP_F(t_i) + (1-x)P_{AF}(t_i), \tag{17}$$

with weight x for F couplings and $1-x$ for AF ones, combined with dimerization in the sense described above (both P_F and P_{AF} are different for even and odd sites). A similar pattern for disorder was proposed in recent numerical studies.[3,4]

We can again map the system onto a random-walk problem with driving force and appropriate barriers. In particular the driving force can be written in terms of the single distribution parameters as

$$F = x\langle \ln[(t_{i_{odd}})^2/(t_{i_{even}})^2]\rangle_F + (1-x)\langle \ln[(t_{i_{odd}})^2(t_{i_{even}})^2]\rangle_{AF}, \tag{18}$$

where *odd* and *even* subindexes indicate the distribution to be used for disorder average.

Notice that even under the strong hypothesis that both single distributions are dimerized (inhomogeneous),

$$\langle \ln[(t_{i_{odd}})^2/(t_{i_{even}})^2]\rangle_F \neq 0$$

and

$$\langle \ln[(t_{i_{odd}})^2(t_{i_{even}})^2]\rangle_{AF} \neq 0,$$

the competition between AF and F couplings can eventually cancel the driving force, under the condition

$$\langle \ln(t^2_{i_{odd}}/t^2_{i_{even}})\rangle_{AF} = x[\langle \ln(t^2_{i_{odd}}/t^2_{i_{even}})\rangle_{AF} - \langle \ln(t^2_{i_{odd}}/t^2_{i_{even}})\rangle_F]. \tag{19}$$

Our detailed analysis corresponds to the general assertion that the transition point is characterized by the condition[14]

$$\langle \ln(t^2_{i_{odd}})\rangle = \langle \ln(t^2_{i_{even}})\rangle. \tag{20}$$

In this sense, similar results were obtained in Ref. 13 for binary distributions.

Equation (19) shows that there are two phases present in the system. For the coupling distribution in Eq. (17) we have that, at least for low magnetic field h, the magnetization follows a power law $M \sim h^{\alpha}$ in most of the parameter space, while there exists a line, with x satisfying Eq. (19), where the magnetization is logarithmic in h, $M \sim \frac{1}{\ln(h^2)^2}$.

It is important to stress that in the power-law regime the dynamical exponent α can be larger or smaller than 1. For the present case it is still given by $2F/D$ where F and D are computed as in Eqs. (15) and (14) but with the binary even and odd distributions in Eq. (17). When the disorder parameter (in this case var$[\ln(t^2)]$) is small and the dimerization is no longer considered, the dynamical exponent turns out to be larger than 1. In contrast, when the disorder is stronger the dynamical exponents take values smaller than 1 and the magnetic susceptibility displays a *singularity* at the origin. It is worth pointing out that this behavior was also reported in RSRG studies in dimerized NN chains.[19]

III. NUMERICAL SELF-CONSISTENT TREATMENT FOR ANTIFERROMAGNETIC NNN SPIN-$\frac{1}{2}$ CHAINS

In this section we consider a spin-$\frac{1}{2}$ XX Hamiltonian in $d=1$ with both NN and NNN AF position-dependent interactions under a uniform magnetic field—namely,

$$H = \sum_{i=1}^{N}[J_i(S_i^xS_{i+1}^x + S_i^yS_{i+1}^y) + J_i'(S_i^xS_{i+2}^x + S_i^yS_{i+2}^y)] - h\sum_{i=1}^{N} S_i^z, \tag{21}$$

where N is the number of spins in the chain and periodic boundary conditions are assumed. The inclusion of NNN couplings does not allow one to apply the analytical procedure used above. We then perform a numerical self-consistent mean-field (SCMF) study of this system.

We first review the procedure proposed in Ref. 15 and then apply it to the present case. In terms of the fermion operators in Eq. (8) this Hamiltonian reads

$$H = \sum_{i=1}^{N}\frac{J_i}{2}[c_i^{\dagger}c_{i+1} + \mathrm{H.c.}] + \sum_{i=1}^{N}\frac{J_i'}{2}[e^{-i\pi\hat{n}_{i+1}}c_i^{\dagger}c_{i+2} + \mathrm{H.c.}] - h\sum_{i=1}^{N}\left(c_i^{\dagger}c_i - \frac{1}{2}\right). \tag{22}$$

First, in order to enable a single-particle treatment of H, we approximate the local fermionic occupation numbers $\hat{n}_i = c_i^{\dagger}c_i$ by their expectation values in an arbitrarily chosen initial state to be varied and determined self-consistently. The local parameters n_i satisfy the constraint $\Sigma_{i=1}^{N}(n_i - 1/2) = m$, with m the system magnetization. Then, in this MF approximation the Hamiltonian can be written as a quadratic form

$$H_{XX}^{(MF)}(\{n_i\}) = \sum_{i,j} c_i^{\dagger}J_{ij}(\{n_i\})c_j, \tag{23}$$

where

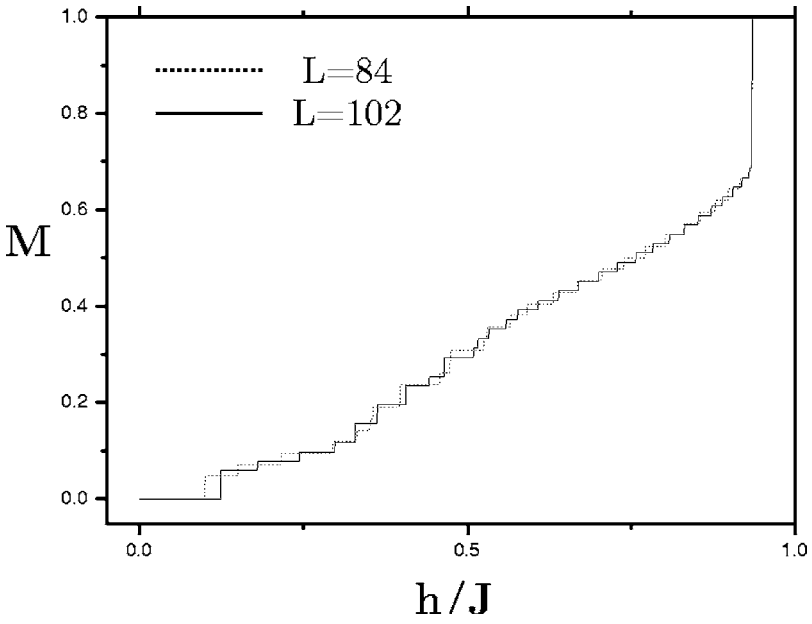

FIG. 2. Magnetization curves for pure chains with $L=102$ and $L=84$ sites both with $J'/J=0.6$. For $M=0$ there is a magnetic plateau.

$$J_{ij}(\{n_i\}) = \begin{cases} \frac{J_i}{2} & \text{if } i,j \text{ are NN,} \\ \frac{J_i'}{2} e^{i\pi n_{i+1}} & \text{if } i,j \text{ are NNN,} \\ 0 & \text{otherwise.} \end{cases}$$

We have omitted the Zeeman term $h\Sigma_{i=1}^{N}(c_i^\dagger c_i - \frac{1}{2})$ as, being diagonal, it can be added later on.

It is our aim to find an approximation to the actual ground state (g.s.) at a given magnetization m. Thus, we estimate this state in the MF Hamiltonian (23) by solving the one-particle spectrum and filling the lowest energy levels to satisfy the constraint $\Sigma_{i=1}^{N}(n_i - 1/2) = m$. Then, we compute a new set of local parameters $n_i' = \langle \text{g.s.}|c_i^\dagger c_i|\text{g.s.}\rangle$ which we use again as input for Eq. (23). Iterating this procedure, we finally obtain a fixed-point configuration of occupation numbers $n_i'(\{n_p\}) = n_p$.

Specifically, the quadratic Hamiltonian can be written in diagonal form

$$H = \sum_{k=1}^{N} \epsilon(k) d_k^\dagger d_k, \tag{24}$$

where the operators c_i are related to d_k by the unitary transformation

$$c_i = \sum_k d_k (Q^\dagger)_{ki}, \tag{25}$$

where Q_{ik} is the matrix of eigenvectors of $J_{ij}(\{n_i\})$. Using standard methods[20] we can easily compute the eigenvalues $\epsilon(k)$ of $H_{XX}^{(MF)}(\{n_i\})$ and eigenvectors Q_{ik} for fairly large spin systems. The set of d_k satisfies fermion anticommutation relations $\{d_k, d_{k'}^\dagger\} = \delta_{k,k'}$ and the total fermion number is conserved

$$N_f = \sum_{i=1}^{N} c_i^\dagger c_i = \sum_{k=1}^{N} d_k^\dagger d_k. \tag{26}$$

So the ground state with magnetization m in the diagonal basis is given by

$$|\text{g.s.}\rangle = \prod_{k=1}^{m+N/2} d_k^\dagger |0\rangle. \tag{27}$$

In this state the energy at zero temperature (for zero magnetic field) is simply given by

$$E_{\text{g.s.}}(m,0) = \sum_{k=1}^{m+N/2} \epsilon(k), \tag{28}$$

whereas for $h \neq 0$ the total energy is shifted as $E_{\text{g.s.}}(m,h) = E_{\text{g.s.}}(m,0) - hm$. The magnetization curve $m(h)$ can finally be obtained by minimizing the energy $E_{\text{g.s.}}(m,h)$ for different given magnetizations.

IV. RESULTS FOR THE PURE CASE

We have tested the SCMF procedure in a pure (ordered) J-J' XX model using chain lengths of up to the order of 100 spins and compared its results with those found by exact diagonalization in smaller chains. In Fig. 2, we show the magnetization behavior under a magnetic field for $J'/J = 0.6$ which clearly indicates the existence of a magnetization plateau at $M=0$.

This initial plateau shows up only in a narrow region of J'/J which in the SCMF approximation was estimated within the bounds $0.55 \lesssim J'/J \lesssim 0.75$. No subsequent plateaus were observed in the system. Notice that in other models (e.g., the XXZ model[11]) there is a plateau at $M=1/3$; however, this not the case in the XX situation.

To lend further support to our SCFM approach, we compared the above results with those obtained in smaller sys-

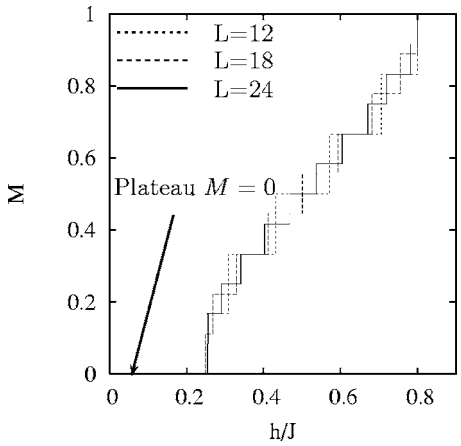

FIG. 3. Magnetization curve for small pure chains with $J'/J=0.6$, obtained by exact diagonalization. There is a clear plateau at $M=0$.

tems using exact diagonalization.[21] In Fig. 3 we exhibit the magnetization curve obtained by the Lanczos technique using chains of 12, 18, and 24 spins, where an $M=0$ plateau also emerges at $J'/J=0.6$. The regime where this plateau appears turns out to be slightly higher than that found with the SCMF approximation. This can be observed in Fig. 4, where we span the magnetic phase diagram. The latter is a compact form of representing conventional magnetization curves in a wide region of coupling parameters. Here, each line stands for a critical field above which the magnetization is increased by flipping one spin. For example, the magnetization plateaus of Fig. 3 are contained completely within a vertical line of Fig. 4 fixed at $J'/J=0.6$ [in passing, it is worth checking out that our saturation fields—highest lines of Fig. 4—closely follow their thermodynamic limit expectations, specifically $h_{sat}/J=1-J'/J$ for $J'/J<1/4$ and $h_{sat}/J=J/(8J')+J'/J$ otherwise]. In agreement with our SCMF expectations, we can see that the first critical field

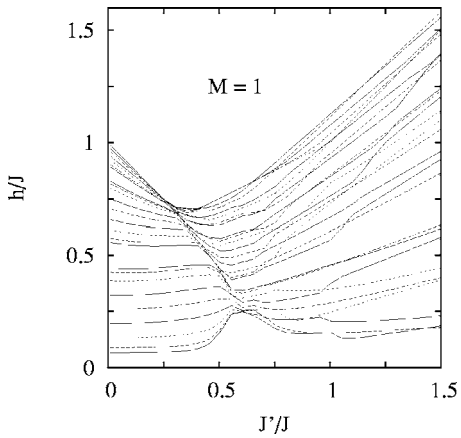

FIG. 4. Magnetic phase diagram for pure chains with $L=24$ (solid lines), 18 (dashed lines), and 12 (dotted lines) spins. As explained in the text, a vertical line at a given value of J'/J contains the whole magnetization curve associated with that parameter. In particular, within the regime $0.5 \lesssim J'/J \lesssim 0.75$ the lowest critical field h_c evidences the appearance of an $M=0$ plateau.

(lowest line of each studied length) is higher in the region $0.5 \lesssim J'/J \lesssim 0.75$ where the $M=0$ plateau is favored and size effects become substantially reduced.

V. RESULTS FOR THE DISORDERED CASE

We now apply the SCMF procedure to our main interest—namely, disordered antiferromagnetic XX chains with a Hamiltonian given by Eq. (21). In this case J_i and J_i' are random NN and NNN coupling exchanges, respectively. For concreteness, let us consider Gaussian distributions of exchanges $P(J_i) \propto e^{-(J_i-\bar{J})^2/2\sigma^2}$ with mean value $\bar{J}=J>0$ for NN couplings, $\bar{J}=J'>0$ for NNN couplings, and the same disorder strength σ in both cases. We explicitly eliminate the negative couplings in the Gaussian tail, so as to work with a totally antiferromagnetic normalized distribution of couplings. We compute numerically the chain magnetization by averaging over many disorder realizations. Typically we considered over 200 samples with periodic boundary conditions and random sets of initial fermionic distributions.

We focused particular attention on low magnetic fields, so as to detect possible singularities near $h=0$ as those observed in disordered NN chains.[18] In Fig. 5 we display the magnetization curve for 102 spins with $J'/J=0.6$ and $\sigma/J=0.5$. Notice that the magnetization plateau observed in the pure case ($\sigma=0$) is now totally suppressed. In fact, all studied values of σ suggest that the plateau of the pure system is unstable under disorder. This observation was also corroborated in smaller systems after diagonalizing them exactly over 100 disorder realizations. In Fig. 6 we show for comparison the magnetization curves obtained for the same values of J, J', and σ. On the contrary, the magnetization remains finite and drops quickly to zero at zero field. Actually, the magnetic susceptibility $\chi=\frac{\partial M}{\partial h}$ exhibits a divergence at $h=0$, as shown in Fig. 5.

A thorough exploration of the mean values of NN and NNN couplings and disorder strength shows that the low-field magnetization curve shows a behavior compatible with a power law $M(h) \sim h^{\alpha}$ in most of the parameter space, except in a small region $J'/J \lesssim 10^{-4}$ where M decreases in a logarithmic form $M \sim \frac{1}{[\ln(h^2)]^2}$. In the power-law region an exponent $\alpha<1$ is obtained for disorder strength $\sigma/J \lesssim 0.3$, corresponding to a singularity in the zero-field magnetic susceptibility. For $\sigma/J \lesssim 0.3$ the magnetization decreases with an exponent α generally larger than 1. Power-law exponents were estimated by fitting the slope in a log-log plot of the magnetization curve, while the logarithmic behavior is clearly observed plotting $M^{-1/2}$ vs $\log(M)$.

In Fig. 7 we show a schematic diagram of our SCMF numerical results. The dashed zone denotes a logarithmic behavior, and the light gray region represents a power-law behavior decrease of M with exponent $\alpha<1$, whereas in the gray zone this exponent is larger than 1. For the ordered case $\sigma=0$ we show a bold line representing the magnetic plateau at $M=0$ within $0.55<J'/J<0.75$.

We can finally compare the low-field behavior of disordered antiferromagnetic NNN chains with those found in disordered NN AF-F chains (Sec. II). We can stress that both

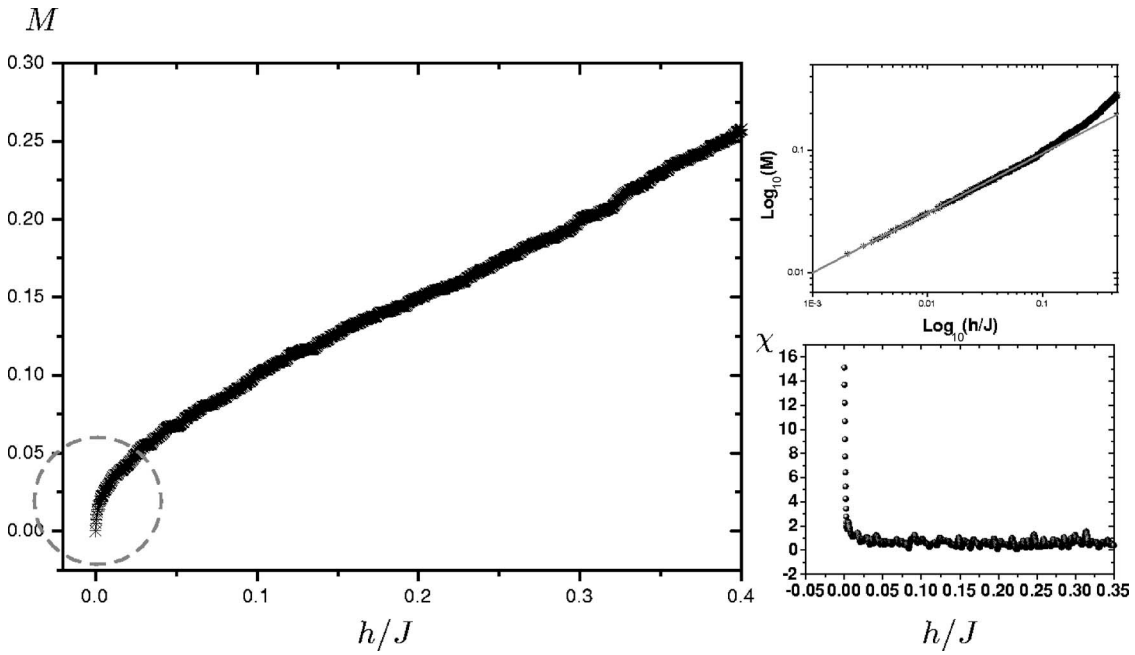

FIG. 5. Magnetization curve for a disordered chain with $L=102$ sites and $J'/J=0.6$, averaged over 150 samples. The magnetization drops quickly to zero, rendering a singular magnetic susceptibility at zero field, as shown in the bottom right panel. In the top right panel we show the corresponding log-log plot and a fit of the slope representing the exponent α. Symbol size in left panel was chosen to represent the error bars.

systems have two phases: a dominant one characterized by a power-law magnetization behavior and a small region of the parameter space where that behavior is close to logarithmic type. Moreover, in the power-law regime both systems can develop singular or smooth zero-field magnetic susceptibilities.

VI. SUMMARY AND CONCLUSIONS

In the first part of this work we studied analytically *XX* spin-$\frac{1}{2}$ chains with random NN interactions, both antiferromagnetic and ferromagnetic, by suitably extending the analysis based on a random-walk problem presented in Ref. 14. We have distinguished three regions in the parameter space with different low-magnetic-field behavior: singular power law $M \propto h^{\alpha}$ with $\alpha<1$, smooth power law with $\alpha>1$, and a logarithmic dependence $\propto \frac{1}{[\ln(h^2)]^2}$. The second part discusses an alternative approach to random antiferromagnetic spin-$\frac{1}{2}$ chains which allows for NN and NNN interactions, using a numerical self-consistent mean-field method adapted from Ref. 15. As for the NN chains analyzed before, we have

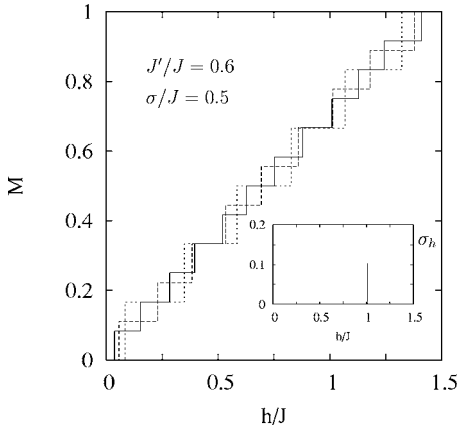

FIG. 6. Exact magnetization curves of disordered chains averaged over 100 samples for $L=24$, 18, and 12 spins (solid, dashed, and dotted lines, respectively; notice that averages were taken over the critical fields, not over the allowed magnetization values, so the curve is not smoothed). J, J', and σ are taken as in Fig. 5. The inset denotes the standard deviations σ_h of the corresponding critical fields.

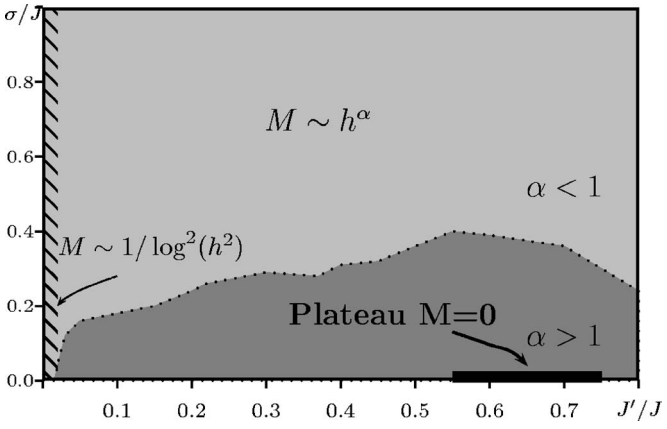

FIG. 7. Schematic diagram of the low-field results obtained for disordered NNN chains. In a tiny (dashed) region the magnetization is logarithmic like. In contrast, in most of parameter space the magnetization follows a power law, with larger disorder leading to singular susceptibility (light gray region) and small disorder leading to smooth magnetization (gray region). A plateau at $M=0$ is present only in the absence of disorder.

found three phases in these systems, the dominant one being a power-law dependence of the magnetization with low external field in most of the parameter space. Also, a logarithmic dependence of the magnetization was found just within a small region of parameters.

Our results show that the two systems have similar low-energy properties. A similar analogy has been found in the study of the same two systems for the Heisenberg [SU(2)] version.[3,4] In both of them there are three phases and most of the parameter space is dominated by a power-law dependence of $M(h)$. Both systems also show a small region where the magnetization displays the same kind of logarithmic singularity. In both systems the power-law region follows a dynamical exponent $\alpha > 1$ for weak disorder, thus yielding a well-behaved magnetic susceptibility. On the contrary, strong disorder yields exponents smaller than 1 and consequently the susceptibility becomes singular at $h=0$. This later behavior has been also found in dimerized spin-$\frac{1}{2}$ chains with disordered NN interactions.[19]

ACKNOWLEDGMENTS

We thank A. Honecker for helpful discussions. This work was partially supported by ECOS-Sud Argentina-France collaboration (Grant No. A04E03), PICS CNRS-CONICET (Grant No. 18294), PICT ANCYPT (Grant No. 20350), and PIP CONICET (Grant No. 5037).

APPENDIX: THE RANDOM-WALK ARGUMENT

In this appendix we summarize the random-walk argument developed in Ref. 14 for studying a disordered quantum chain. We consider the disordered one-dimensional tight-binding spinless fermion model

$$H = \sum_{i=1}^{N} t_i (c_i^\dagger c_{i+1} + c_{i+1}^\dagger c_i), \tag{A1}$$

related to XX spin chains as described in Sec. II. The hopping amplitudes t_i follow a given position-independent probability distribution $P(t_i)$. The aim of the argument is to relate the spectral distribution of one-particle states of this system to $P(t_i)$.

As a first step one looks for one-particle solutions of the Schrödinger equation in the form

$$|\psi\rangle = \sum_i u_i c_i^\dagger |0\rangle, \tag{A2}$$

with energy E. For the state coefficients u_i one finds the recurrence relation

$$u_{i-1} J_{i-1} + u_{i+1} J_i = E u_i, \tag{A3}$$

which after changing variables to

$$\Delta_i \equiv u_{i-1} t_{i-1} / u_i \tag{A4}$$

reads

$$\Delta_{i+1} = \frac{J_i^2}{(E - \Delta_i)}. \tag{A5}$$

The key ingredient, proved in Ref. 17, is that the last term Δ_N in the sequence can be parametrized by a phase monotonically increasing with E, so that the number of eigenstates with energy below E satisfying appropriate boundary conditions is given by the number of positive terms in the sequence $\{\Delta_i\}$. We call $N_{1p}(E)$ the ratio between this number and the number of sites in the chain. The sequence is indeed evident for $E=0$: $\{\Delta_i\}$ follows the alternating pattern $+-+-+-+-\cdots$, and $N_{1p}(E=0)=0.5$.

The second step is then to describe the sequence $\{\Delta_i\}$ for low energies. We start with $E=0$, where we can concentrate only in the positive terms—say, at even sites—and analyze their magnitude. Iterating Eq. (A5) and taking logarithms we have

$$\ln(\Delta_{2i}) = \ln[(t_{2i-1}/t_{2i-2})^2] + \ln(\Delta_{2i-2}), \tag{A6}$$

so that the variable $v_{2i} \equiv \ln(\Delta_{2i})$ describes a random walk with drift force $\ln[(t_{2i-1}/t_{2i-2})^2]$ and the position index $2i$ as time evolution parameter. Moreover, since the probability distribution for t_i is translation invariant, the average displacement is zero,

$$\langle v_{2i} - v_{2i-2} \rangle = 0, \tag{A7}$$

while the average squared displacement is given by

$$\langle (v_{2i} - v_{2i-2})^2 \rangle = \langle \{\ln[(t_{2i-1}/t_{2i-2})^2]\}^2 \rangle \equiv 2\sigma^2. \tag{A8}$$

In the thermodynamic limit $N \to \infty$, the random-walk problem can be represented by a diffusion process. One approximates the index $2i$ by a continuous variable t and introduces $\phi(v,t)$ as the probability density for $v(t)$. This probability density follows the diffusion equation

$$2\frac{\partial \phi(v,t)}{\partial t} = \sigma^2 \frac{\partial^2 \phi(v,t)}{\partial v^2}. \tag{A9}$$

Using these results we can now analyze the sequence $\{\Delta_i\}$ for small $E > 0$. Iterating Eq. (A5) one finds

$$\Delta_{2i} = \left(\frac{t_{2i-1}}{t_{2i-2}}\right)^2 \Delta_{2i-2} \frac{(1 - E/\Delta_{2i-2})}{1 + \dfrac{(E\Delta_{2i-2} - E^2)}{t_{2i-2}^2}}. \tag{A10}$$

Under the conditions

$$E \ll \Delta \ll t_{2i-2}^2 / E, \tag{A11}$$

one gets essentially the random-walk behavior in Eq. (A6). Then v follows a random walk in the range

$$\ln(E) \ll v \ll \ln(\tilde{t}^2/E), \tag{A12}$$

where $\tilde{t}$ is the average value of the distribution $\{t_i\}$. This situation can be approximately described as a random walk with barriers: a quick analysis of signs in Eq. (A10) shows that the lower one, at $\Delta_{2i} \approx E$, is an absorbing barrier while the upper one, at $\Delta \approx \tilde{t}^2/E$, is a reflecting barrier. The stochastic evolution for Δ_i can be thus depicted as the following cycles: Δ alternates signs with random magnitude; whenever

Δ gets close to $\tilde{t}^2/E$, it simply "reflects" down, but when it gets close to E, it is "absorbed," in the sense that sign alternation is broken, a double sign $++$ shows up, and the magnitude of the altered positive term is of the order of $\tilde{t}^2/E$. The number of positive terms Δ_i is then $N/2$ plus the number of complete cycles ending in the absorbing barrier.

As the last step, we calculate the average value $\bar{n}$ of steps necessary for completing a cycle. The barriers can be implemented by boundary conditions on the diffusion process as

$$\left(\frac{\partial \phi}{\partial v}\right)_{v=v_{max}} = 0 \tag{A13}$$

and

$$\phi|_{v=v_{min}} = 0, \tag{A14}$$

where v_{min} and v_{max} are the limits for v in Eq. (A12). Let

$$P(n) = \int_{v_{min}}^{v_{max}} \phi(v,t)dv \tag{A15}$$

be the probability that v remains between v_{min} and v_{max}; then, $\bar{n}$ can be computed as

$$\bar{n} = \int_0^\infty n\left(-\frac{dP}{dn}\right)dn. \tag{A16}$$

It is straightforward to obtain

$$\bar{n} = \frac{(\Delta v)^2}{\sigma^2}, \tag{A17}$$

where $\Delta v = v_{max} - v_{min}$.

Counting positive signs in the sequence $\{\Delta_i\}$ renders $N_{1p}(E)$ as

$$N_{1p}(E) - N_{1p}(0) = N_{1p}(E) - \frac{1}{2} = \frac{1}{2\bar{n}}. \tag{A18}$$

The result in Eq. (A17) allows us to give expressions for the integrated density of states,

$$N_{1p}(E) \cong \frac{1}{2}\left(1 + \frac{\sigma^2}{[\ln(\tilde{J}/E)^2]^2}\right), \tag{A19}$$

and normalized density of states,

$$\rho(E) = \frac{dN_{1p}(E)}{dE} \cong \frac{2\sigma^2}{E}\frac{1}{[\ln(\tilde{J}/E)^2]^3} \cong \frac{2\sigma^2}{E|\ln E^2|^3}. \tag{A20}$$

Extensions of the above argument to nonhomogeneous distributions are provided in the main text.

[1] See, for example, T. Giamarchi, *Quantum Physics in One Dimension* (Clarendon Press, Oxford, 2004).
[2] F. Iglói and C. Monthus, Phys. Rep. **412**, 277 (2005).
[3] J. A. Hoyos and E. Miranda, Phys. Rev. B **69**, 214411 (2004).
[4] E. Yusuf and K. Yang, Phys. Rev. B **68**, 024425 (2003).
[5] R. Mélin, Y. C. Lin, P. Lajkó, H. Rieger, and F. Iglói, Phys. Rev. B **65**, 104415 (2002).
[6] C. Dasgupta and S. K. Ma, Phys. Rev. B **22**, 1305 (1980).
[7] D. Fisher, Phys. Rev. B **50**, 3799 (1994).
[8] See E. Westerberg, A. Furusaki, M. Sigrist, and P. A. Lee, Phys. Rev. B **55**, 12578 (1997) and references therein.
[9] A. Furusaki, M. Sigrist, P. A. Lee, K. Tanaka, and N. Nagaosa, Phys. Rev. Lett. **73**, 2622 (1994).
[10] T. Hikihara, A. Furusaki, and M. Sigrist, Phys. Rev. B **60**, 12116 (1999).
[11] K. Okunishi and T. Tonegawa, J. Phys. Soc. Jpn. **74**, 151 (2005).
[12] P. Henelius and S. M. Girvin, Phys. Rev. B **57**, 11457 (1998).
[13] F. Igloi, R. Juhász, and H. Rieger, Phys. Rev. B **61**, 11552 (2000).
[14] T. P. Eggarter and R. Riedinger, Phys. Rev. B **18**, 569 (1978).
[15] D. C. Cabra and G. L. Rossini, Phys. Rev. B **69**, 184425 (2004).
[16] P. Jordan and E. P. Wigner, Z. Phys. **47**, 631 (1928).
[17] H. Schmidt, Phys. Rev. **105**, 425 (1957).
[18] D. C. Cabra, A. De Martino, M. D. Grynberg, S. Peysson, and P. Pujol, Phys. Rev. Lett. **85**, 4791 (2000).
[19] R. A. Hyman, K. Yang, R. N. Bhatt, and S. M. Girvin, Phys. Rev. Lett. **76**, 839 (1995).
[20] W. Press, W. Vetterling, S. A. Teukolsky, and B. P. Flannery, *Numerical Recipes in C: The art of scientific computing* (Cambridge University Press, Cambridge, England, 1992).
[21] See, for instance, G. H. Golub and C. F. van Loan, *Matrix Computations*, 3rd ed. (Johns Hopkins University Press, Baltimore, 1996).